sustainability

MDPI

Article

Resilience Assessment of an Urban Metro Complex Network: A Case Study of the Zhengzhou Metro

Qingjie Qi [1], Yangyang Meng [1,*], Xiaofei Zhao [2] and Jianzhong Liu [3]

[1] Institute of Emergency Science Research, Chinese Institute of Coal Science, Beijing 100013, China
[2] Department of Computer Science, City University of Hong Kong, Kowloon, Hong Kong, China
[3] China Coal Technology & Engineering Group, Beijing 100013, China
* Correspondence: mengyy17@tsinghua.org.cn

Abstract: An urban metro network is susceptible to becoming vulnerable and difficult to recover quickly in the face of an unexpected attack on account of the system's complexity and the threat of various emergencies. Therefore, it is necessary to assess the resilience of urban metro networks. However, the research on resilience assessment of urban metro networks is still in the development stage, and it is better to conduct said research using a technique which combines many attributes, multiple methods, and several cases. Therefore, based on the complex network modeling and topological characteristics analysis of metro systems, a metro network's robustness and vulnerability measurement method under node interruption and edge failure is proposed for the first time in this study. Then, considering the three cases of general station interruption, interchange station interruption, and traffic tunnel failure, a quantitative resilience assessment model of metro networks is put forward, and the corresponding recovery strategies are discussed. Finally, a case study of the Zhengzhou Metro Network (ZZMN) under an extreme rainstorm is conducted to demonstrate the viability of the proposed model. The results show that ZZMN possesses scale-free and small-world network properties, and it is robust to random interruptions but vulnerable to deliberate attacks. ZZMN still needs to improve its effectiveness in information transmission. The centrality distribution for each node in the ZZMN network differs significantly, and each node's failure has a unique impact on the network. The larger the *DC*, *BC*, and *PR* of a node is, the lower the network's robustness after its removal is, and the stronger the vulnerability is. Compared with the three cases of general station interruption, interchange station interruption, and traffic tunnel failure, the network loss caused by tunnel failure was the lowest, followed by general station interruption, and the interruption at interchange stations was the most costly. Given the failures under various cases, the metro management department should prioritize selecting the optimal recovery strategy to improve the resilience of the metro network system. This study's findings can assist in making urban metro systems less vulnerable to emergencies and more resilient for a quick recovery, which can provide scientific theoretical guidance and decision support for the safety and resilient, sustainable development of urban metro systems.

Keywords: urban metro network; complex topology; robustness; vulnerability; resilience assessment

Citation: Qi, Q.; Meng, Y.; Zhao, X.; Liu, J. Resilience Assessment of an Urban Metro Complex Network: A Case Study of the Zhengzhou Metro. *Sustainability* **2022**, *14*, 11555. https://doi.org/10.3390/su141811555

Academic Editors: Wen Yi, Xinyuan Chen, Di Huang and Shuaian Wang

Received: 6 August 2022
Accepted: 9 September 2022
Published: 15 September 2022

1. Introduction

As an essential part of all urban traffic activities, the urban metro network plays a vital role in the sustainable development of modern cities [1–3]. The metro network system is a complex network composed of multiple nodes and edges, and its topology structure forms the cornerstone of how it functions [4–7]. Nowadays, with the rapid and flourishing development of metro construction in cities all over the world, metro networks are increasingly being developed. According to the Survey of Urban Rail Transit Lines in Mainland China in the first half of 2022, which was released by the China Association of Metro, up to 30 June 2022, 51 cities in mainland China had put into operation 9573.65 km

of rail transit lines, and metro lines were 7529.02 km of them, accounting for 78.64% of the total. Chinese urban rail transit has entered a new era of interconnection and network-based operation [8].

The complexity of the metro network structure and the interaction of different lines and functions make the metro system face various disruption threats (such as typhoons, rainstorms, earthquakes, equipment breakdowns, and terrorist attacks) in daily operation, which have a significant impact on the punctuality and safety of passenger transportation [9,10]. For instance, the Zhengzhou Metro suffered an extreme rainstorm disaster on 20 July 2021, resulting in a terrible flooding tragedy that killed 14 people and injured 5 others. This emergency triggered great concern and reflection on the whole society [11,12]. Faced with such a drastic disturbance threat, the vulnerability [13] of a metro network system is significantly enhanced, and it needs to have a strong absorption capacity and rapid recovery ability to reduce losses. That aside, the resilience theory [14] runs through the system's whole life cycle and emphasizes the system's adaptive ability and learning ability, which can better capture changes in the system's performance both before and after a disruption. The robustness [15], vulnerability [16], recovery [17], reliability [18], and other capacities of the system may all be fully understood by a resilience assessment based on the resilience theory. The vulnerable areas can also be located early, allowing for the implementation of targeted resilience-improving interventions.

As a result, numerous professionals and academics began to study the robustness and vulnerability of metro systems. The robustness [19] of a system is the ability to tolerate perturbations that might affect the system's functional body, and the vulnerability [20] refers to the quality or state of being exposed to the possibility of being attacked or harmed. The current research on the robustness and vulnerability of metro networks is mainly carried out in the following ways. (1) The metro network's variations in system performance in the event of a disruption or attack are investigated using complex network theory or graph theory [21–24]. (2) Using big data, the effects of emergencies on metro passenger flow are examined [25–27]. (3) Passenger flow, vehicle flow, and other factors are taken into account when building a metro-weighted network model to analyze the resistance ability and damage implications of the metro network system under disturbance events [15,28,29].

In the meantime, the robustness and vulnerability research techniques currently in use mostly concentrate on theoretical analysis, simulation, mathematical modeling, and data-driven methods. Among them, theoretical analysis involves the definitions, related concepts, and quantitative indicators of robustness and vulnerability [30,31]. The major goal of the simulation is to represent the cascading failure of the metro network system brought on by disturbances or attacks from unforeseen events (such as terrorist attacks or natural disasters) [16,32,33] which may have happened or may not have occurred. In mathematical modeling, indicators (such as network efficiency, the maximum connected subgraph, the shortest path length, connectivity, and passenger flow distribution) are proposed for quantitative calculation, and a mathematical model is developed to assess the metro network's robustness and vulnerability [29,34–36]. The development of metro intelligence and information has a study trend called the data-driven technique [37–39], which is still in the exploration phase. It primarily gathers large amounts of data about factors such as passenger flow, traffic flow, cell phone signals, videos, and photos. In summation, we may learn how well the metro system can withstand both internal and external disturbances as well as the extent of the damage.

The study of metro resilience is currently a popular topic in the field of metro safety, based on the robustness and vulnerability of the metro. However, metro network resilience, which varies depending on the research scope and attributes, still lacks a uniform concept and definition [40–43]. Some studies distinguish resilience from stability and emphasize that it focuses on recovery, while others stress that resilience should be present throughout the whole life cycle of the system. According to this study, a system's resilience is a process attribute or a time-varying attribute which necessitates consideration of the entire process, including what happens before, during, and after disruptions occur, as well as the system

status at various stages. Nevertheless, the ultimate objective is to quickly bring the system to a relatively stable and acceptable level. Some academics have outlined some resilience-related ideas (such as reliability, adaptability, redundancy, rapidity, recoverability, and survivability) [44,45]. While each notion has a specific focus, resilience is more inclusive and general.

Currently, the studies on metro network resilience focus mostly on developing some assessment indexes, which can be divided into three categories. The first is resilience indexes based on metro topology [46,47], which emphasize the structural characteristics of the network system. The second category is resilience indexes based on some related attributes [48–50]. The common attribute-based resilience index is Robustness, Redundancy, Resourcefulness, and Rapidity (4R). The interference phase is represented by the robustness and redundancy, whereas the recovery phase is represented by the resourcefulness and rapidity. The recovery stage is the focus of resilience research at present. The third category is resilience indexes based on the system's functioning [51–53]. This means that the metro system's resilience may be assessed by using its performance or function during the entire disturbance process. In order to accomplish this, mathematical modeling of the system function $Q(t)$ is typically necessary. Resilience indexes based on the system's functioning, which have time-varying properties and effectively describe the supply, demand, response, and recovery of the metro system under disruption, surpass the limits of the first two indices in comparison. Many academics are increasingly paying attention to them. A resilience assessment based on the metro network's system performance modeling will also be conducted in this study.

The studies mentioned above show that the present research on the robustness and vulnerability assessment of metro networks has produced significant findings. Studies on metro network resilience are still in the development stage and tend to concentrate on a single element, one method, or one particular example, while the combination of several characteristics, methods, and cases can compensate for the shortcomings of a single situation. Metro network resilience can be studied comprehensively based on the topology characteristics, robustness, and vulnerability analysis results. This can deepen our awareness of a metro network's sustainable development, enabling us to take swift, efficient action to lessen severe repercussions and significant losses in the event of an emergency.

According to this background, based on the complex network modeling and topological characteristic analysis of metro systems, the robustness and vulnerability measurement method of metro networks under node interruption and edge failure is put forward for the first time by the simulation in this paper. Then, combined with the theory of resilience loss triangle, a quantitative resilience assessment model of metro networks is proposed, and the corresponding recovery strategies are discussed for three cases: general station interruption, interchange station interruption, and traffic tunnel failure. Finally, an empirical study is conducted on the case of the Zhengzhou Metro Network under an extreme rainstorm, which demonstrates the effectiveness of the proposed model and method.

This study's practical usefulness is highlighted by the following in particular. First of all, the investigation of the complex topological features of the metro network in this study can help transport planners and policy makers comprehend the structural complexity of a metro network and the differences in importance distribution between all metro stations. Second, we can clearly determine which stations have a greater impact on the metro network after failure and which stations have a higher vulnerability from the robustness and vulnerability measurement results. This information allows the metro management department to develop targeted policies and put in place appropriate safety supervision measures for these stations. Finally, based on the findings of the metro network's resilience assessment, they can comprehend the optimal recovery strategies under the three cases of common station interruption, transfer station interruption, and tunnel failure, enabling them to respond quickly and effectively to major disasters in the future while minimizing losses to the greatest extent possible. On the other hand, for urban metro networks under construction (such as the Zhengzhou Metro), transport planners and policy makers can

learn from the existing operation and management of metro networks to carry out sustainable planning and construction for future lines so as to improve the operation and service level of the entire metro network. The related study results are helpful for lowering the metropolitan metro network's vulnerability to emergencies and boosting its resilience for quick recovery. This study can provide scientific theoretical guidance and decision support for the safety and resilient sustainable development of urban metro systems, which has significant practical implications.

2. Methodology

2.1. Complex Network Modeling and Topological Index Measurement of a Metro System

A complex network is composed of many nodes and connections between the nodes, while metro stations and lines between the stations make up a metro network. Considering the analogy between complex network and metro network as well as the characteristics of several classical spatial models of complex networks (such as Space L, Space P, Space B, and Space C) [54], the Space L model was selected to conduct the complex topology model $G = (N, E)$ for the metro network in this study to restore the authenticity of the metro network, and $N = \{v_i, i = 1, 2, \cdots, N\}$ was the set of nodes (i.e., the metro stations). $E = e_{ij}, i, j = 1, 2, \cdots, N, i \neq j$ was the set of edges, and $e_{ij} = (v_i, v_j)$ represented a connection consisting of two adjacent nodes (i, j) (i.e., a line in the metro). The Space L model emphasizes whether nodes i and j are adjacent. If so, there will be an associated adjacency matrix $A = [a_{ij}]$, where $a_{ij} = 1$; otherwise, $a_{ij} = 0$.

In complex networks, the node centralities (such as the degree centrality (*DC*), eigenvector centrality (*EC*), betweenness centrality (*BC*), closeness centrality (*CC*), and PageRank (*PR*)) are often used to measure the roles and effects of different nodes in the network [55–57]. In urban rail transit networks, node centrality describes the degree to which a station is associated with other stations throughout the entire system. This study also chose several widely used node centralities to measure the importance of nodes and the topological characteristics of a network. The specific definitions and calculation formulae are shown in Table 1.

Table 1. The definitions and calculations of node centralities in complex networks.

Index	Definition	Formula
DC [58]	*DC* is the total number of the connected edges of a node.	$k_i = \sum_j^N a_{ij}, DC_i = \frac{k_i}{N-1}$
EC [58]	*EC* can identify the different effects of neighbors of a node on it.	$\lambda e_i = \sum_{j=1}^N a_{ij} e_j, e = [e_1, e_2, \cdots, e_n]^T$
BC [59]	*BC* is the shortest number of paths through a node.	$BC_i = \sum_{i \neq j \neq k} \frac{\sigma_{jk}(i)}{\sigma_{jk}}$
CC[59]	*CC* is used to measure the ability of a station to affect another node through the network.	$CC_i = \frac{N-1}{\sum_{j=1, i \neq j}^N d_{ij}}$
PR [60]	*PR* is used to calculate the ranking of nodes in *G* based on the structure of incoming links.	$PR_i = (1-\lambda)\frac{1}{n} + \lambda \sum_{j:j \to k} \frac{PR_j}{d_j}, \lambda \in [0, 1]$

In addition to some node centralities, the following indicators are commonly used to measure the topological characteristics of complex networks: the network diameter D, average shortest path length *APL*, network connectivity β, network density ρ, and network efficiency *Eff*. Their corresponding meanings and calculation methods are shown in Table 2, where N and E are the number of network nodes and connected edges, respectively, and d_{ij} is the distance between nodes i and j. Aside from that, δ (degree_assortativity_coefficient) reveals the level of network coordination and is used to measure the similarity of links [61]. The values of δ vary in the range of $[-1, 1]$. When $\delta \in [0, 1]$, the network is assortative. This means that in the network, high-degree nodes prefer to be linked to other high-degree nodes, and low-degree nodes tend to be linked to other low-degree nodes. In contrast, the

network is disassortative when $\delta \in [-1, 0]$, which means that the high-degree nodes are more likely to connect to the nodes with low degrees.

Table 2. The definitions and calculations of network topological indexes.

Index	Definition	Formula
D	The maximum distance between any two nodes in a network.	$D = \max d_{ij}$
APL	The average of the shortest distances between all pairs of nodes.	$APL = \frac{1}{N(N-1)} \sum_{i \neq j} d_{ij}$
β	The connectivity degree of a network.	$\beta = \frac{E}{3N-6}$
ρ	The intensive degree of a network.	$\rho = \frac{2E}{N(N-1)}$

2.2. Robustness and Vulnerability Measurement of a Metro Network

For the metro system, there will be inevitable emergencies (such as vehicle failure, signal failure, power failure, and deliberate attacks) in daily operation, which will lead to the suspension of stations or lines or even interruption of the whole network. Then, the metro network's capacity for connectivity and the effectiveness of information transmission will inevitably suffer as a result. Numerous professionals and academics have started looking into the reliability of the metro network to help ease this reduction. Robustness describes a metro network's capacity to withstand disruption and continue information transmission in the event of an emergency. A system with strong robustness means that the system has strong resistance to accidents. Vulnerability refers to the degradation of network connectivity performance and the severity of system loss after the network encounters an emergency.

Here, we put forward the key index for a complex network: network efficiency (*Eff*). *Eff* is used to measure the ability to transmit information [23,24,46], which is global in this study. *Eff* is also used to characterize the connectivity between network nodes. The calculation formula of *Eff* is shown in Equation (1), and it is in the range of [0, 1]. *APL* and *Eff* can represent the global transmission capability of the network. The shorter the *APL* is, the higher the *Eff* is, and the faster the information transfer rate between nodes is.

In the event of an attack on the metro network, node connectivity is jeopardized, making the network vulnerable. Through the removal of nodes and connecting edges, the actual station interruption and tunnel failure are simulated in this study. Although partial failures [62,63] are typical in daily metro operations, this analysis exclusively took cases of complete failures into account. Then, the network efficiency would become a new one: Eff'. Two modes of node failure were set as a random attack and intentional attack. This study assumes that all stations are subject to an equal probability of random attack, while an intentional attack targets those nodes that are more important to the network. In these two modes, robustness reflects the new network connectivity of the metro network after removing nodes or edges. Therefore, robustness can be measured quantitatively by Equation (3). Vulnerability measures the decline and damage degree of the connectivity performance of the metro network, which can be described by the change in network efficiency ΔEff [46], as shown in Equation (4).

For the random attack, the simulation process set-up in this study was as follows. For all nodes, one was randomly removed each time until the last one, and the new network efficiency Eff' after each removal was calculated and updated. The specific process of a random attack on the nodes is shown in Figure 1a. For the intentional attack, only one node was removed each time in the order of *node_id*, and the number of nodes was $N - 1$. The network efficiency Eff_i' after node i was removed could be calculated correspondingly. Figure 1b shows the specific process of an intentional attack on the nodes.

With relative simplicity, we could remove the edge between i and j to simulate a tunnel failure. Furthermore, the robustness and vulnerability could be calculated according to the corresponding formula to measure the impact of the tunnel failure on the network:

$$Eff = \frac{1}{N(N-1)} \sum_{i \neq j} \frac{1}{d_{ij}} \tag{1}$$

$$Eff' = \frac{1}{N'(N'-1)} \sum_{i \neq j} \frac{1}{d'_{ij}} \tag{2}$$

$$R(Robustness) = Eff' \tag{3}$$

$$V(Vulnerability) = Eff - Eff' \tag{4}$$

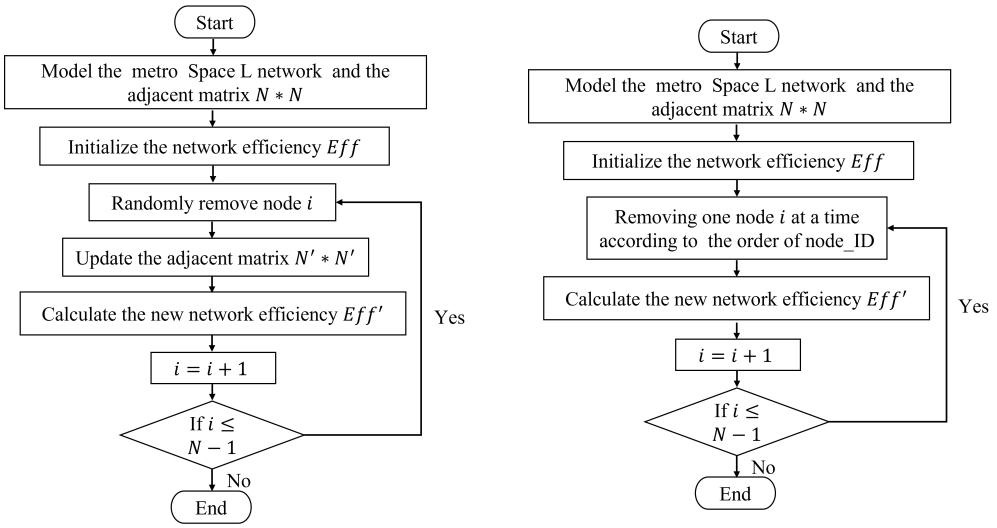

Figure 1. (**a**) The simulation process of a random attack on a node. (**b**) The simulation process of an intentional attack on a node.

2.3. Resilience Assessment Modeling of a Metro Network

Figure 2 shows the variation trend of the system performance $Q(t)$ of the metro network under an attack over time. The $Q(t)$ of the metro network defined in this study can be quantitatively expressed by the network connectivity, as in the network efficiency *Eff*. The initial network performance of the metro network was $Q(t_0)$, and $Q(t)$ plunged precipitously to a low point at t_0 following the attack. According to the robustness and vulnerability measurement of the metro network in Section 2.2, it can be concluded that the network performance corresponding to the time t_0 is the network robustness level, and the reduced network performance $\Delta Q(t)$ is the network vulnerability under this attack. From t_0, a series of response measures were taken, and the network performance began to recover gradually. After the period t_h, the network reached a state of full recovery at t_1. It should be mentioned that different recovery times were difficult to calculate because of the station's complex condition in the actual world. Therefore, the corresponding time under various recovery sequences was the same, according to our proposed resilience evaluation methodology.

In this study, the resilience *Re* of the metro network system is defined as the recovery capability after an emergency attack (as shown in the orange shaded part of Figure 2), which can be calculated by Equation (5). The definite integral $\int_{t_0}^{t_1} Q(t)dt$ can be obtained by the trapezoidal sum method, Monte Carlo method, shoelace Gaussian area formula, etc. Since the data involved in this study were discrete, the trapezoidal sum method was chosen to roughly estimate the area of the shaded part. In addition, there existed resilience loss in the failure-response-recovery process, namely the resilience loss triangle, as shown in the green shaded part of Figure 2, which can be calculated quantitatively by Equation (6).

Based on Section 2.2, we can supplement the mathematical expressions of robustness and vulnerability as shown in Equations (7) and (8):

$$Re = \frac{\int_{t_0}^{t_1} Q(t)dt}{t_h Q(t_0)} = \frac{\int_{t_0}^{t_1} Eff(t)dt}{t_h Eff_0} \tag{5}$$

$$Re_{loss} = \int_{t_0}^{t_1} [Q(t_0) - Q(t)]dt \tag{6}$$

$$R = Q(t)_{\min} = Eff' \tag{7}$$

$$V = Q(t_0) - Q(t)_{\min} = Eff - Eff' \tag{8}$$

In Section 2.2, the station and tunnel failures are simulated by removing the corresponding node and edge. Based on this, the resilience assessment modeling of a metro network under node and edge failures can be carried out. The following three cases are described.

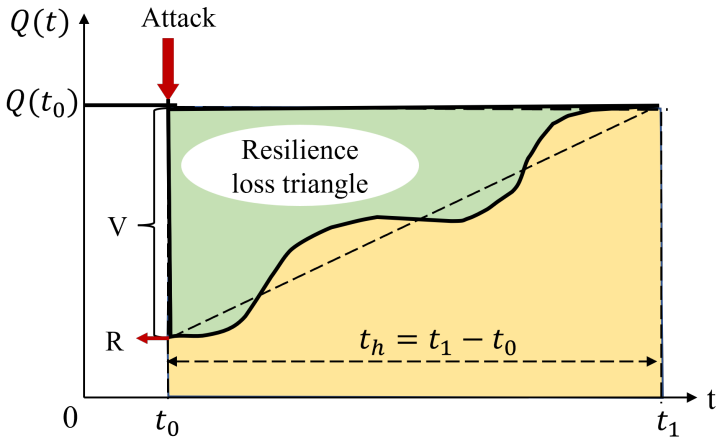

Figure 2. Resilience assessment model of metro network under attack.

Case 1: General station interruption

In a metro system, a general station is one where lines cannot be changed to other lines. For a general station failure, the specific process can be illustrated by Figure 3a. Stations A, B, and C are three adjacent general stations on Line 1. Stage (1) is the normal operation state, and in stage (2), station A is interrupted and cannot be connected with B or C. Stage (3) is the recovery process, and there are two types: e1 → e2 and e2 → e1; that is, the connection sequence is between A and B as well as A and C. Stage (4) is the complete recovery to the state in stage (1). The whole process from node failure to complete recovery is rather straightforward for general stations. Combined with the resilience assessment model and the calculation of relevant parameters, the robustness, vulnerability, resilience, and resilience loss of general stations after disruption can be quantitatively assessed.

Case 2: Interchange station interruption

The metro network is more severely affected when interchange stations fail than general stations are. Taking the two-line interchange station A as an example, Figure 3b depicts the whole process from interruption to recovery. Station A is connected to four other stations in stage (1), which is the initial normal state. When station A is interrupted after deliberate attack, it will present as stage (2) and will be disconnected from the other four stations. From this moment forward, the response measures are taken to recovery. Since station A owns four linked edges, there will be $A_4^4 = 24$ recovery sequences. Furthermore, we can conclude that there are A_{2n}^{2n} restoration sequences for an n-line interchange station. Network resilience varies under different recovery sequences. The corresponding $Q(t)$ and network resilience indexes can be obtained for each recovered sequence by combining

Figure 2 and Equations (5)–(8). By comparing the network resilience in different sequences, the optimal network recovery strategy can be obtained to improve the effectiveness of network recovery.

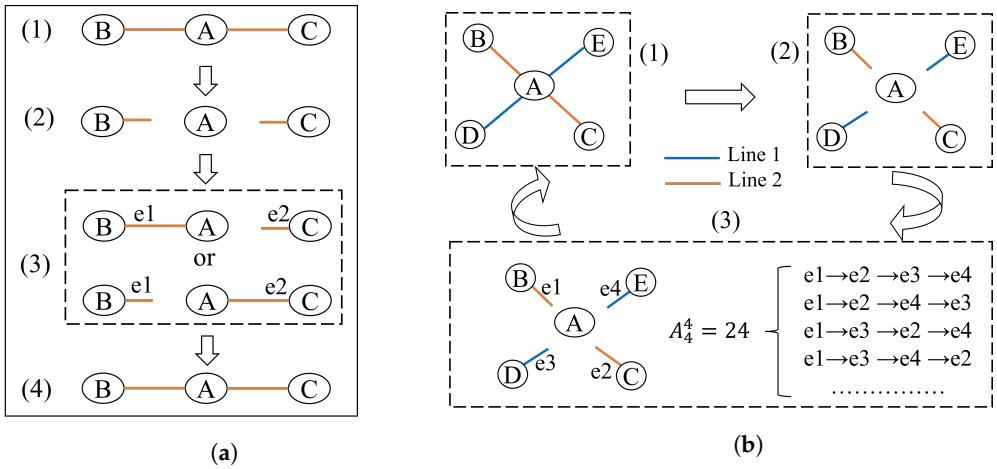

(**a**) (**b**)

Figure 3. (**a**) Schematic diagram of recovery process under general station interruption. (**b**) Schematic diagram of recovery process under interchange station interruption.

Case 3: Tunnel failure

Tunnel failure in a metro network is represented by the removal of the connection between a node pair (i, j). As shown in Figure 4, stages (2) and (3) describe the failure process of edge (A, B). The total number of nodes N remains the same, and the Eff' can be calculated after removing the connected edge. The recovery process can be simulated by appending the connection between (A, B), and network efficiency is the initial Eff_0. Similarly, the corresponding network resilience indexes under tunnel failure can be calculated by combining Figure 2 and Equations (5)–(8).

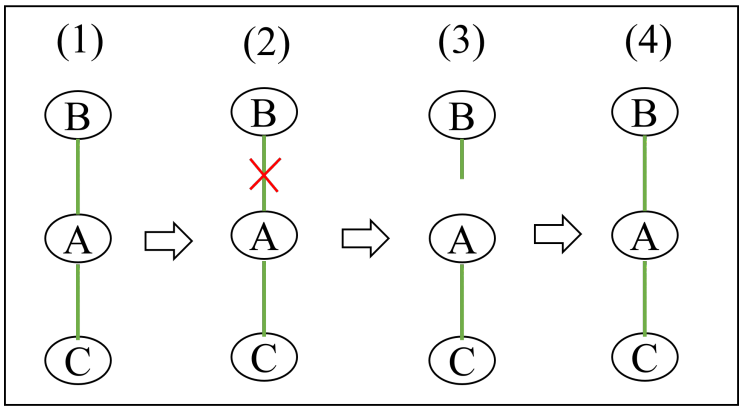

Figure 4. Schematic diagram of recovery process under metro tunnel failure.

3. Case Study: Zhengzhou Metro Network

On 28 December 2013, Line 1 (L–1) of the Zhengzhou Metro (ZZM) was opened, making it the first urban rail transit system in Henan province and the 17th overall on the Chinese mainland. Up to July 2022, Zhengzhou Metro has opened a total of seven lines (L–1, 2, 3, 4, 5, 14, and Chengjiao) with an operation length of 215.5 km and owns a total of 131 stations, including 17 two–line interchange stations.

According to the line number sequence, all stations can be coded successively. For instance, the ID of Henan University of Technology station on L–1 is 0, followed by Zhengzhou University Sci–Tech Park station (ID = 1). For the interchange stations, they are coded with a smaller line number. For example, the ID of the Tielu station on L–1 is 5, and

it will be skipped on L–14. Thus, all stations of the Zhengzhou Metro in 2021 can be coded from 0 to 130, as shown in Figure 5.

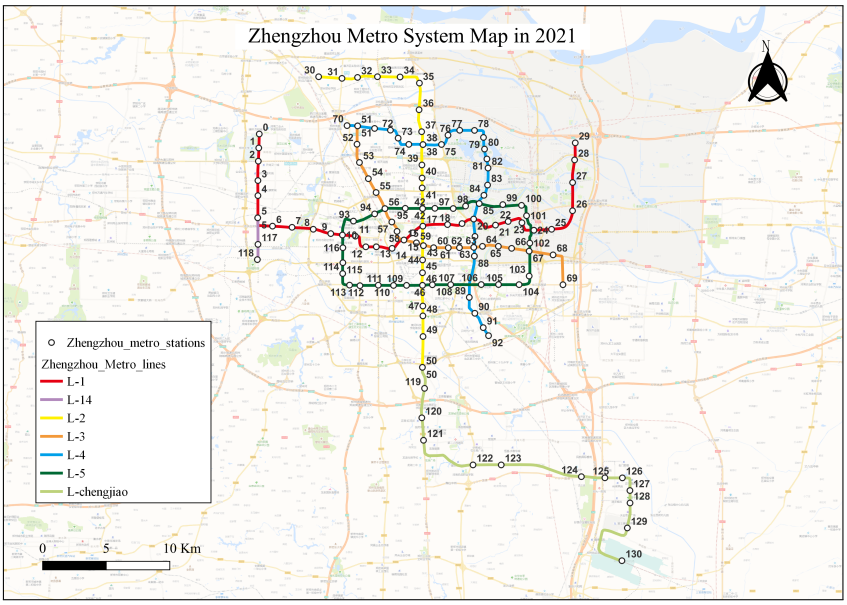

Figure 5. ZZMN in 31 December 2021.

3.1. Complex Topological Characteristic Analysis

Based on Section 2.1, the topological structure and node centrality characteristics of the ZZMN can be quantitatively analyzed. The basic information of the ZZMN is shown in Table 3, from which it can be seen that the ZZMN has 131 nodes and 142 undirected edges. The average degree $\overline{k}$ is 2.168, and the maximum degree is 4. The highest proportion of nodes with $k = 2$ occupies the highest proportion of 81.68%, indicating that a small number of nodes with a larger degree take up the critical positions in the network. The fitting result of the cumulative degree was a power-law distribution $p(k) = 20.82\ \mathrm{k}^{-4.47}$, and the fitting accuracy was $R^2 = 0.977$. The fitting curve shows a straight line in the *log-log* coordinate system, indicating that the ZZMN characterizes a scale-free network. Combined with the properties of scale-free networks [28,46,64], it can be concluded that the ZZMN is robust to random interruptions but vulnerable to deliberate attacks.

Table 3. The basic topological indexes of the ZZMN.

Indexes	Values	Indexes	Values
N	131	ρ	0.0167
E	142	δ	−0.105
$\overline{k}$	2.168	$\overline{DC}$	0.0181
C	0	$\overline{EC}$	0.0531
D	35	$\overline{BC}$	0.0952
APL	11.77	$\overline{CC}$	0.0920
β	0.367	$\overline{PR}$	0.0081

The APL and D of the ZZMN were 11.77 and 35, respectively. The density and connectivity degree of the ZZMN were $\rho = 0.0167$ and $\beta = 0.367$, respectively. The clustering coefficient C measures the local clustering of the network or the local efficiency of information transmission and represents the possibility that the neighbors of a node i are neighbors of each other. The C of the ZZMN was zero, indicating that the local efficiency among nodes was a little bit low. At present, the ZZMN is in the process of construction and development, and the network efficiency is being improved. According to the literature [46],

if a network meets two conditions of $APL > \ln(N)/\ln(\bar{k})$ and $C < \bar{k}/N$, it will be a small-world network. For the ZZMN, we could obtain the results of $\ln(N)/\ln(\bar{k}) = 6.30 < 11.77$ and $\bar{k}/N = 0.0166 > 0$, so it can be concluded that the ZZMN characterizes a small-world network. The δ (degree_assortativity_coefficient) was -0.105, and the ZZMN is disassortative, indicating that nodes with a high degree tend to connect with ones with a low degree, and nodes with a low degree tend to be connected to ones with a high degree.

Figure 6 displays the centrality distributions of each node based on an understanding of the topological properties of the ZZMN. Among the five centralities, *BC* and *CC* accounted for the largest proportion on the whole, while *PR* accounted for the lowest proportion. Comparatively speaking, the nodes with the largest *DC* were 14 two-line interchange stations with $k = 4$. The *EC* and *CC* of Zijingshan Station (ID = 17) were the largest among all nodes, which were 0.421 and 0.133, respectively. Huanghelu Station (ID = 42) owned the largest BC with 0.393, while Henan Orthopaedics Hospital Station (ID = 67) had the largest PR of 0.013. Table 3 shows the average values of the different centralities of all nodes. Among them, $\overline{BC}$ and $\overline{CC}$ were larger than the others, while $\overline{PR}$ of the ZZMN was only 0.0081.

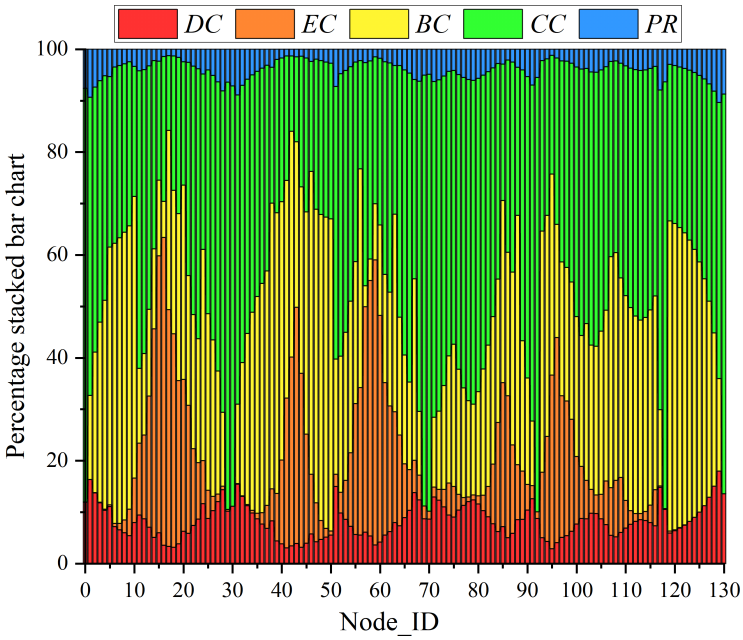

Figure 6. The distributions of node centralities in the ZZMN.

3.2. Robustness and Vulnerability Assessment

The number of nodes in the ZZMN was $N = 131$, and d_{ij} could be obtained by the *Dijkstra* algorithm [64]. According to Equation (1) for network efficiency, the Eff_0 of the ZZMN under normal operation is 0.1320. Based on the measurement method of robustness and vulnerability of metro networks in Section 2.2, the *R* and *V* of the ZZMN subjected to different failures can be calculated and discussed.

Case 1: Node interruption

Node interruption can be divided into two types: (1) random attacks and (2) intentional attacks.

(1) Random attacks

According to the simulation flow chart of network cascade failure in Figure 1a, one node is randomly selected from all nodes for removal, with the next one being chosen similarly, and this process continues until only one node remains. The results for network efficiency obtained by this simulation method have a certain randomness. In order to acquire the declining trend of network effectiveness along with the proportion of eliminated nodes, as shown in Figure 7, we performed the simulation 10 times at random. Figure 7a

shows the results of 10 random simulations, and Figure 7b shows their mean results. The number of network nodes decreased as the percentage of eliminated nodes rose, and the *Eff* steadily decreased. Figure 7b shows that the network efficiency fell from 0.1320 to 0.0269 when the eliminated nodes made up 55.73% of the network; that is, the robustness at the time was 20.35% of the initial efficiency, indicating that the ZZMN has certain robustness to random interruptions, which is also demonstrated by the characteristics of a scale-free network.

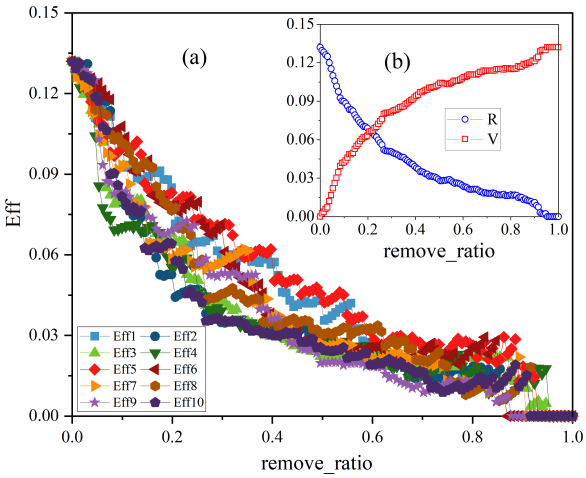

Figure 7. The robustness and vulnerability of the ZZMN after removing nodes randomly: (**a**) All results of 10 random simulations and (**b**) The mean results of 10 random simulations.

(2) Intentional attacks

All nodes of the ZZMN were removed in accordance with the sequence of *node_ID*, and the corresponding network efficiency Eff' could be obtained for different nodes. By combining Equations (3) and (4), we could obtain the network robustness and vulnerability corresponding to intentional attacks on different nodes. As shown in Figure 8, various node failures had different effects on the network. Among them, Nanwulibao (ID = 46) is a two–line interchange station, and Xinzheng International Airport (ID = 130) is a general station. After removing the Nanwulibao station, the network possessed the lowest robustness $R_{\min} = 0.1135$ and the highest vulnerability $V_{\max} = 0.0185$. Meanwhile, the network robustness reached the highest value $R_{\max} = 0.133$ after removing the Xinzheng International Airport station, which had a network efficiency Eff_0 even larger than the original one. In addition, the network vulnerability was larger after the removal of interchange stations compared with removing general stations, demonstrating that interchange stations have stronger impacts on the network. Therefore, the metro management department should strengthen the safety supervision of interchange stations.

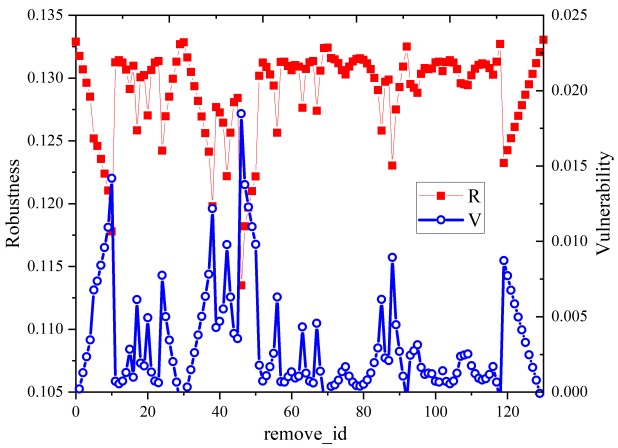

Figure 8. The robustness and vulnerability of the ZZMN under intentional attacks.

Combined with the difference in node centrality of the ZZMN in Section 3.1, we measured the impacts of node failure under different centralities by removing the node with the largest centrality index. After removing Zijingshan Station (ID = 17), which had the largest *EC* and *CC*, the *APL* of the ZZMN rose to 12.46, and the *D* went up to 38. The network assortativity δ became worse, the *Eff* decreased to 0.126, and the vulnerability *V* was 0.006. Nevertheless, when we removed the Huanghelu station, which had the largest *BC*, the *APL* of the ZZMN increased to 13.33, and the *D* increased from 35 to 42. The network robustness and vulnerability were $R = 0.122$ and $V = 0.010$, respectively. As can be observed, the effects of removing related nodes for various centrality indexes on the network varied significantly. To evaluate the relationships between the robustness *R*, vulnerability *V*, and node centralities (*DC*, *EC*, *BC*, *CC*, and *PR*), Pearson correlation analysis was conducted, and the results are shown in Figure 9. It can be seen that R was negatively correlated with *V*, *DC*, *BC*, and *PR*. The *P* value was at a 0.01 level (two–tailed), showing significant correlation. In other words, the network was less robust and more vulnerable when the nodes with bigger *DC*, *BC*, and *PR* values were removed.

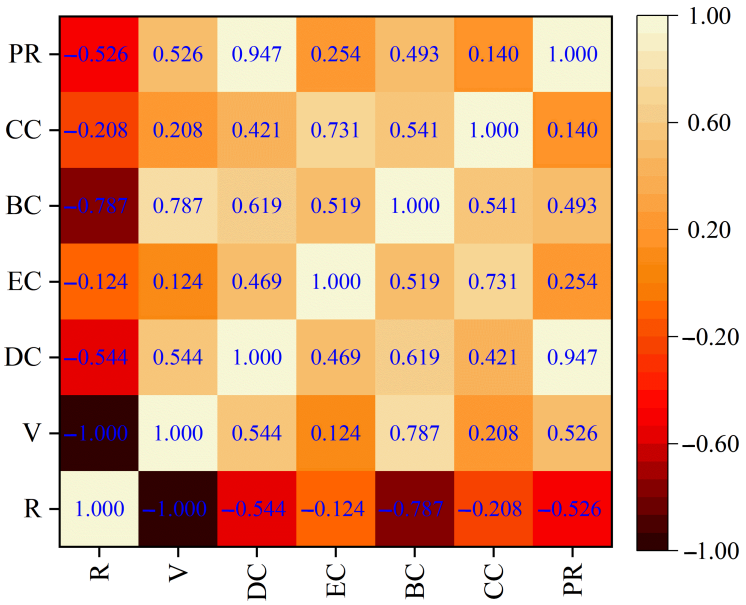

Figure 9. The heat map of correlation analysis.

Case 2: Tunnel failure

This study used the extreme rainstorm event that hit the Zhengzhou Metro on 20 July 2021 as its research background for tunnel failure. The extreme rainstorm caused a large amount of water to break down the retaining wall of the entrance line and enter the tunnel between the Haitansi station (ID = 56) and Shakoulu station (ID = 94) of Line 5, leading to the subsequent tragedy. In this context, this study simulated the metro tunnel failure by removing the edge between nodes ID = 56 and ID = 94, and the basic network indicators obtained are shown in Table 4. The *D* of the ZZMN after tunnel failure remained the same, and the *APL* increased from 11.77 to 12.18, indicating that the average shortest path of the network became longer and the cost of network travel rose. In addition, the fact that connectivity β decreased from 0.367 to 0.364 also proved this. Network density ρ barely changed, and the assortativity δ increased from -0.105 to -0.087, indicating that the broken ZZMN was still disassortative. Moreover, the network efficiency *Eff* decreased from 0.132 to 0.1288. Combined with the definition of robustness and vulnerability in this study, we could obtain the results of $R = 0.1288$ and $V = 0.0032$. This displays the effects of the traffic tunnel failure between the Haitansi station and Shakoulu station on the ZZMN network.

Table 4. The basic indexes of the ZZMN after tunnel failure.

Indexes	Values	Indexes	Values
N	131	ρ	0.0167
E	141	δ	−0.087
D	35	Eff'	0.1288
APL	12.18	R	0.1288
β	0.364	V	0.0032

3.3. Resilience Assessment

Based on Sections 2.3 and 3.2, we can achieve the quantitative resilience assessment of the ZZMN under different scenarios. The extreme rainstorm event in the ZZMN was selected as the research background, where the accident locations were the Shakoulu station (a general station) and Haitansi station (a two–line interchange station). Therefore, we set the following three cases. Case 1 is the recovery strategy and resilience assessment under the interruption of a general station (Shakoulu). Case 2 discusses the optimal recovery strategy and resilience measurement of an interchange station (Haitansi) interruption. In Case 3, resilience assessment is carried out based on a traffic tunnel failure between the Shakoulu station and Haitansi station.

Case 1: General station interruption

In this case, the interruption simulation was run at the Shakoulu station during an extreme rainstorm. Between Yuejigongyuan Station (ID = 93) and Haitansi Station (ID = 56) is Shakoulu Station (ID = 94). When combined with the recovery flow chart in Figure 3a and the resilience assessment model in Figure 2, the trend chart of the network performance of Shakoulu Station over time in the process of an extreme rainstorm could be obtained (seen in Figure 10). The initial network performance was $Q_0 = Eff_0 = 0.1320$, and it changed to $Q_1 = Eff_1 = 0.1273$ after removing Shakoulu Station. According to Figure 3a, there are two recovery strategies: (93,94) → (94,56) and (94,56) → (93,94). If the edge (93,94) is recovered first, then the network performance is $Q_2 = Eff_2 = 0.1288$, while it will be $Q_2' = Eff_2' = 0.1292$ if we initially recover the edge (94,56). In both cases, the network performance was finally restored to Q_3 = 0.1320. Therefore, the network resilience of the above two recovery strategies can be calculated to be $Re_1|_{i=94} = 0.9790$ and $Re_2|_{i=94} = 0.9805$, respectively, and the corresponding resilience losses are $Re_{loss1}|_{i=94} = 0.0056$ and $Re_{loss2}|_{i=94} = 0.0052$, respectively. In contrast, $Re_2|_{i=94}$ was larger. It can be determined that the Shakoulu station's optimal network recovery strategy involved recovering the first edge (94,56) before recovering the second edge (93,94), and the resilience attained in this circumstance was the highest:

$$Re_1|_{i=94} = \frac{Q_1 + 2Q_2 + Q_3}{2 \times 2Q_0} = \frac{0.1273 + 2 \times 0.1288 + 0.1320}{4 \times 0.1320} = 0.9790 \quad (9)$$

$$Re_2|_{i=94} = \frac{Q_1 + 2Q_2' + Q_3}{2 \times 2Q_0} = \frac{0.1273 + 2 \times 0.1292 + 0.1320}{4 \times 0.1320} = 0.9805 \quad (10)$$

$$Re_{loss1}|_{i=94} = \frac{4Q_0 - (Q_1 + 2Q_2 + Q_3)}{2} = \frac{4 \times 0.1320 - (0.1273 + 2 \times 0.1288 + 0.1320)}{2} = 0.0056 \quad (11)$$

$$Re_{loss2}|_{i=94} = \frac{4Q_0 - (Q_1 + 2Q_2' + Q_3)}{2} = \frac{4 \times 0.1320 - (0.1273 + 2 \times 0.1292 + 0.1320)}{2} = 0.0052 \quad (12)$$

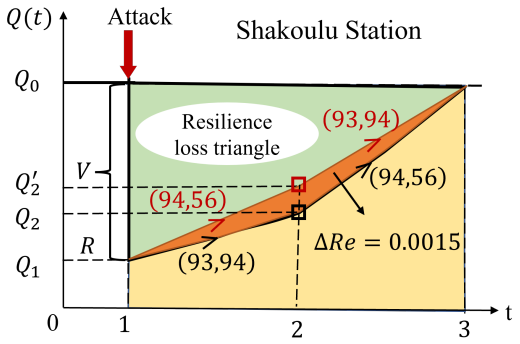

Figure 10. The recovery strategy after the failure of Shakoulu Station.

Case 2: Interchange station interruption

As shown in Figure 11, Haitansi Station (ID = 56) is the interchange station of L–3 and L–5, which also suffered heavy losses in the extreme rainstorm disaster on 20 July 2021. In L–3, it is adjacent to Nanyangxincun Station (ID = 55) and Dashiqiao Station (ID = 57), and in L–5, it is between Shakoulu Station (ID = 94) and Zhengzhou People's Hospital Station (ID = 95). It is shown in Figure 11a that the Haitansi station has four connected edges, and we define e1, e2, e3, and e4 as the connected edges (55,56), (56,57), (93,56), and (56,95), respectively. The network performance under the failure of Haitansi Station was $Q_1 = 0.1237$. Therefore, the network robustness was $R = 0.1237$, and the vulnerability was $V = Q_0 - Q_1 = 0.0083$. According to Figures 2 and 3b, we could obtain a total of $A_4^4 = 24$ recovery sequences. Thus, the network efficiency and performance could be measured in each sequence, and the results are displayed in Table 5.

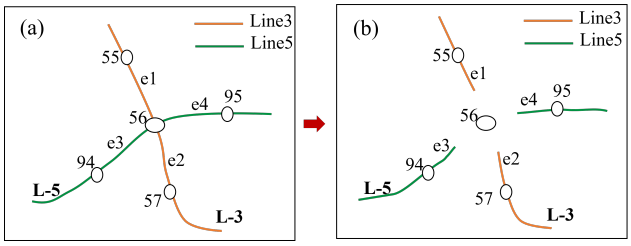

Figure 11. The schematic diagram of the failure of Haitansi Station: (**a**) Before failure and (**b**) After failure.

Table 5. The network performance of different recovery edges under the failure of Haitansi Station.

Edge	$Q(t)$	Edge	$Q(t)$	Edge	$Q(t)$	Edge	$Q(t)$	Edge	$Q(t)$	Edge	$Q(t)$
e1	0.1248	e1	0.1248	e1	0.1248	e1	0.1248	e1	0.1248	e1	0.1248
e2	0.1274	e2	0.1274	e3	0.1270	e3	0.1270	e4	0.1280	e4	0.1280
e3	0.1291	e4	0.1288	e2	0.1291	e4	0.1311	e2	0.1288	e3	0.1311
e4	0.1320	e3	0.1320	e4	0.1320	e2	0.1320	e3	0.1320	e2	0.1320
e2	0.1254	e2	0.1254	e2	0.1254	e2	0.1254	e2	0.1254	e2	0.1254
e1	0.1274	e1	0.1274	e3	0.1262	e3	0.1262	e4	0.1260	e4	0.1260
e3	0.1291	e4	0.1288	e1	0.1291	e4	0.1285	e1	0.1288	e3	0.1285
e4	0.1320	e3	0.1320	e4	0.1320	e1	0.1320	e3	0.1320	e1	0.1320
e3	0.1251	e3	0.1251	e3	0.1251	e3	0.1251	e3	0.1251	e3	0.1251
e1	0.1270	e1	0.1270	e2	0.1262	e2	0.1262	e4	0.1280	e4	0.1280
e2	0.1291	e4	0.1311	e1	0.1291	e4	0.1285	e1	0.1311	e2	0.1285
e4	0.1320	e2	0.1320	e4	0.1320	e1	0.1320	e2	0.1320	e1	0.1320
e4	0.1256	e4	0.1256	e4	0.1256	e4	0.1256	e4	0.1256	e4	0.1256
e1	0.1280	e1	0.1280	e2	0.1260	e2	0.1260	e3	0.1280	e3	0.1280
e2	0.1288	e3	0.1311	e1	0.1288	e3	0.1285	e1	0.1311	e2	0.1285
e3	0.1320	e2	0.1320	e3	0.1320	e1	0.1320	e2	0.1320	e1	0.1320

One of the sequences e1-e2-e3-e4 is given as an example. The network performance after recovering e1 was $Q_2 = 0.1248$, and it changed to $Q_3 = 0.1274$ after recovering e2 and then $Q_4 = 0.1291$ after recovering e3. Finally, the complete network emerged after restoring e4 (i.e., $Q_5 = Q_0 = 0.1320$). Based on the network performance acquired in each step, the trend of $Q(t)$ in this sequence can be clearly known. Thus, we could calculate the network resilience $Re_1|_{i=56}$ and resilience loss $Re_{loss1}|_{i=56}$ under this recovery strategy. Similarly, we could obtain the resilience results under 24 recovery sequences, as shown in Table 6. Comparatively speaking, when the recovery sequence was e4-e1-e3-e2, the resilience reached its maximum of $Re_{\max}|_{i=56} = 0.9710$, while it would be at its minimum $Re_{\min}|_{i=56} = 0.9619$ when the recovery sequence was e3-e2-e4-e1, as shown in Figure 12. Hence, for Haitansi Station, the optimal recovery strategy was (56,95)→ (55,56)→ (93,56)→ (56,57) after its interruption, and the resilience loss attained its lowest value $Re_{loss\min}|_{i=56} = 0.0153$:

$$Re_1|_{i=56} = \frac{Q_1 + 2(Q_2 + Q_3 + Q_4) + Q_5}{2 \times 4Q_0} = 0.9644 \quad (13)$$

$$Re_{loss1}|_{i=94} = \frac{8Q_0 - [Q_1 + 2(Q_2 + Q_3 + Q_4) + Q_5]}{2} = 0.0188 \quad (14)$$

Table 6. The network resilience of different recovery sequences under the failure of Haitansi Station.

Sequence	*Re*	Sequence	*Re*	Sequence	*Re*
e1-e2-e3-e4	0.9644	e2-e3-e1-e4	0.9633	e3-e4-e1-e2	0.9700
e1-e2-e4-e3	0.9639	e2-e3-e4-e1	0.9623	e3-e4-e2-e1	0.9652
e1-e3-e2-e4	0.9637	e2-e4-e1-e3	0.9625	e4-e1-e2-e3	0.9667
e1-e3-e4-e2	0.9676	e2-e4-e3-e1	0.9620	e4-e1-e3-e2	0.9710
e1-e4-e2-e3	0.9651	e3-e1-e2-e4	0.9644	e4-e2-e1-e3	0.9629
e1-e4-e3-e2	0.9695	e3-e1-e4-e2	0.9683	e4-e2-e3-e1	0.9625
e2-e1-e3-e4	0.9655	e3-e2-e1-e4	0.9628	e4-e3-e1-e2	0.9710
e2-e1-e4-e3	0.9650	e3-e2-e4-e1	0.9619	e4-e3-e2-e1	0.9661

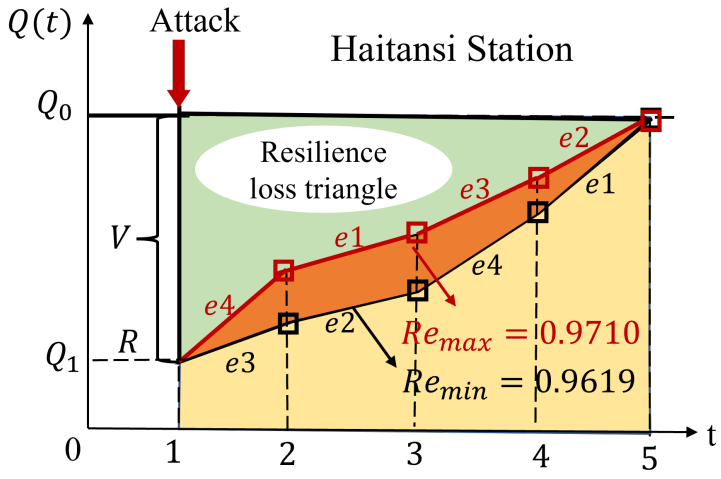

Figure 12. The optimal and worst recovery strategies under the failure of Haitansi Station.

Case 3: Tunnel failure

The resilience assessment could be completed based on the robustness and vulnerability measurement related to the metro tunnel failure in Section 3.2. The scenario where the traffic tunnel between Haitansi (ID = 56) and Shakoulu stations (ID = 94) was hit by the extreme rainstorm disaster continued to be selected. The initial network performance was $Q_0 = 0.1320$, and it was $Q_1 = 0.1288$ after the failure. The recovery was relatively simple; that is, the network would become complete again by adding the connecting

edges between (94,56). Therefore, $Q_2 = Q_0 = 0.1320$. Network resilience in this case was $Re|_{(94,56)} = (Q_1 + Q_2)/(2Q_0) = (0.1288 + 0.1320)/(2 \times 0.1320) = 0.9880$, and the resilience loss was $Re_{loss}|_{(94,56)} = [2Q_0 - (Q_1 + Q_2)]/2 = 0.0016$.

In the three failure cases listed above, the network loss caused by the tunnel failure was the least severe, followed by the general station disruption. Additionally, the disruption at the interchange station had the greatest financial impact on the network. To prevent the serious situation of interchange station failure, the metro management department should strengthen the safety supervision and management of the interchange stations in daily operation.

4. Conclusions and Future Works

Due to the system complexity and the threat of various emergencies, urban metro networks are susceptible to becoming vulnerable and difficult to recover quickly in the face of unexpected attacks. Therefore, it is essential to study the urban metro network system's resilience. Based on complex network modeling and topological characteristic analysis of urban metro networks, the robustness and vulnerability measurement of a metro network under different failure cases are given in this study. The resilience assessment models of a metro network under different failure cases were constructed, and the corresponding resilience recovery strategies were compared and discussed. In addition, taking the Zhengzhou Metro when it was hit by an extreme rainstorm disaster on 20 July 2021 as an example, the application research was carried out. The following conclusions can be drawn:

(1) The ZZMN is a scale-free complex network which is robust to random interruptions but vulnerable to deliberate attacks. At present, the ZZMN is in the construction and development process, the local efficiency between nodes is lower, and there is room for improvement in the network information transmission efficiency. The ZZMN characterizes a small-world network, and it is disassortative. Additionally, the roles and effects that various nodes have in the network vary substantially, as does the distribution of centrality among them. Among the five centralities (*DC*, *EC*, *BC*, *CC*, and *PR*) distributions, *BC* and *CC* accounted for the largest proportions, while PR had the lowest.

(2) The robustness and vulnerability measurement results show that network efficiency declined from 0.1320 to 0.0269 when the ratio of deleted nodes was 55.73%, indicating that the ZZMN had certain robustness to random node interruption. The intentional attack's simulation findings demonstrate that different node failures had various impacts on the network. The larger the *DC*, *BC*, and *PR* of the node was, the lower the network robustness was after its removal, and the stronger the vulnerability was. The network vulnerability was the greatest and the robustness was the lowest after the removal of Nanwulibao Station. Compared with the general stations, the network vulnerability was higher after removal of the interchange stations. Therefore, the metro management department should strengthen the safety supervision of interchange stations.

(3) The metro network was restored in two steps for general station interruptions and in A_{2n}^{2n} steps for station interruptions at n-line interchanges. For Shakoulu Station, it was optimal to restore Shakoulu–Haitansi first and Yuejigongyuan–Shakoulu later, and the resilience was 0.9805 at this condition. For Haitansi Station, network resilience could reach the maximum value of 0.9710 according to the optimal recovery strategy, and the resilience loss was minimal at 0.0153. What is more, network resilience under the traffic tunnel failure between the Haitansi and Shakoulu stations was 0.9880. The network loss during tunnel failure was the least of the three failure cases, followed by general station interruption. Interruptions at the interchange stations had the greatest financial impact on the network.

Based on the complex topological characteristics of metro networks, this study evaluated the robustness, vulnerability, and resilience under different failure cases and gave the

optimal recovery strategy under the corresponding cases. This study helps to improve the metro network's resilience and reduce its vulnerability to emergencies. However, there are still some spaces to be further studied. For example, this study does not take into account elements such as traffic flow, environmental considerations, or passenger movement. In future works, we will establish a weighted metro network based on the above factors to study the dynamic resilience of urban metro networks. At the same time, more variables and scenarios will be considered further to optimize the proposed resilience assessment model of the metro network. Additionally, the resilience effects of partial node failure on the network structure and traffic flow provide another fascinating topic for research.

Author Contributions: Conceptualization, Y.M. and Q.Q.; methodology, Y.M.; software, Y.M. and X.Z.; writing—original draft, Y.M.; writing—review and editing, Y.M. and X.Z.; visualization, Y.M. and X.Z.; supervision, Q.Q. and J.L.; funding acquisition, Q.Q. and J.L. All authors have read and agreed to the published version of the manuscript.

Funding: This research was funded by the Innovation and Entrepreneurship Science and Technology Project of the Chinese Institute of Coal Science (No.2021-JSYF-006), and the Innovation and Entrepreneurship Science and Technology Project of the China Coal Technology and Engineering Group (No.2022-2-QN004).

Institutional Review Board Statement: Not applicable.

Informed Consent Statement: Not applicable.

Data Availability Statement: Not applicable.

Conflicts of Interest: The authors declare no conflict of interest.

Abbreviations

The following abbreviations are used in this manuscript:

N	The number of nodes
E	The number of edges
$\overline{k}$	The average value of the node degree
C	The clustering coefficient of the network
D	The diameter of the network
δ	The degree_assortativity_coefficient of the network
DC	The degree centrality
EC	The eigenvector centrality
BC	The betweenness centrality
CC	The closeness centrality
PR	The PageRank centrality
$\overline{DC}$	The average value of DC
$\overline{EC}$	The average value of EC
$\overline{BC}$	The average value of BC
$\overline{CC}$	The average value of CC
$\overline{PR}$	The average value of PR
Eff	The network efficiency
Eff'	The new network efficiency

References

1. Tu, Q.; Zhang, Q.; Zhang, Z.J.; Gong, D.; Tang, M.C. A Deep Spatio-Temporal Fuzzy Neural Network for Subway Passenger Flow Prediction with COVID-19 Search Engine Data. *IEEE Trans. Fuzzy Syst.* **2022**, 1. [CrossRef]
2. Ma, M.; Hu, D.; Chien, S.I.J.; Liu, J.; Yang, X.; Ma, Z. Evolution Assessment of Urban Rail Transit Networks: A Case Study of Xi'an, China. *Phys. A Stat. Mech. Its Appl.* **2022**, *603*, 127670. [CrossRef]
3. Wen, S.; Shi, J.; Zhang, W. Impact of Urban Rail Transit Network on Residential and Commercial Land Values in China: A Complex Network Perspective. *Complexity* **2021**, *2021*, 8849066. [CrossRef]
4. González, S.H.; De La Mota, I.F. Applying Complex Network Theory to the Analysis of Mexico City Metro Network (1969–2018). *Case Stud. Transp. Pol.* **2021**, *9*, 1344–1357. [CrossRef]

5. Li, X.; Zhang, P.; Zhu, G. Measuring Method of Node Importance of Urban Rail Network Based on H Index. *Appl. Sci.* **2019**, *9*, 5189. [CrossRef]
6. Zhang, Y.; Tu, L. Characteristic Analysis and Important Stations Identification of Wuhan Metro Complex Network Based on Two Models. In Proceedings of the 2022 14th International Conference on Advanced Computational Intelligence (ICACI), Wuhan, China, 15–17 July 2022; pp. 370–375. [CrossRef]
7. Pu, H.; Li, Y.; Ma, C. Topology Analysis of Lanzhou Public Transport Network Based on Double-Layer Complex Network Theory. *Phys. A Stat. Mech. Its Appl.* **2022**, *592*, 126694. [CrossRef]
8. Gu, J.; Jiang, Z.; Sun, Y.; Zhou, M.; Liao, S.; Chen, J. Spatio-Temporal Trajectory Estimation Based on Incomplete Wi-Fi Probe Data in Urban Rail Transit Network. *Knowl. Based Syst.* **2021**, *211*, 106528. [CrossRef] [PubMed]
9. Wu, H.W.; Li, E.Q.; Sun, Y.Y.; Dong, B.T. Research on the Operation Safety Evaluation of Urban Rail Stations Based on the Improved TOPSIS Method and Entropy Weight Method. *J. Rail Transp. Plan. Manag.* **2021**, *20*, 100262. [CrossRef]
10. Huang, W.; Shuai, B.; Sun, Y.; Wang, Y.; Antwi, E. Using Entropy-TOPSIS Method to Evaluate Urban Rail Transit System Operation Performance: The China Case. *Transp. Res. Part A Policy Pract.* **2018**, *111*, 292–303. [CrossRef]
11. Xu, Q.; Han, L.; Xu, K. Causal Analysis and Prevention Measures for Extreme Heavy Rainstorms in Zhengzhou to Protect Human Health. *Behav. Sci.* **2022**, *12*, 176. [CrossRef]
12. Zhao, X.; Li, H.; Qi, Y. Are Chinese Cities Prepared to Manage the Risks of Extreme Weather Events? Evidence from the 2021.07.20 Zhengzhou Flood in Henan Province. *SSRN Electron. J.* **2022**. [CrossRef]
13. Sun, D.; Zhao, Y.; Lu, Q.C. Vulnerability Analysis of Urban Rail Transit Networks: A Case Study of Shanghai, China. *Sustainability* **2015**, *7*, 6919–6936. [CrossRef]
14. Wei, S.; Pan, J. Resilience of Urban Network Structure in China: The Perspective of Disruption. *ISPRS Int. J. Geo-Inf.* **2021**, *10*, 796. [CrossRef]
15. Gao, C.; Fan, Y.; Jiang, S.; Deng, Y.; Liu, J.; Li, X. Dynamic Robustness Analysis of a Two-Layer Rail Transit Network Model. *IEEE Trans. Intell. Transp. Syst.* **2021**, *23*, 6509–6524. [CrossRef]
16. Wang, Y.; Tian, C. Measure Vulnerability of Metro Network Under Cascading Failure. *IEEE Access* **2021**, *9*, 683–692. [CrossRef]
17. Saadat, Y.; Ayyub, B.M.; Zhang, Y.; Zhang, D.; Huang, H. Resilience-Based Strategies for Topology Enhancement and Recovery of Metrorail Transit Networks. *ASCE-ASME J. Risk Uncertain. Eng. Syst. Part A Civ. Eng.* **2020**, *6*, 04020017. [CrossRef]
18. Kim, H.; Song, Y. An Integrated Measure of Accessibility and Reliability of Mass Transit Systems. *Transportation* **2018**, *45*, 1075–1100. [CrossRef]
19. Wikipedia Contributors. Robustness. 2022. Available online: https://en.wikipedia.org/wiki/Robustness (accessed on 15 June 2022).
20. Wikipedia Contributors. Vulnerability. 2022. Available online: https://en.wikipedia.org/wiki/Vulnerability (accessed on 15 June 2022).
21. Zhang, J.; Wang, S.; Wang, X. Comparison Analysis on Vulnerability of Metro Networks Based on Complex Network. *Phys. A Stat. Mech. Its Appl.* **2018**, *496*, 72–78. [CrossRef]
22. Zhang, J.; Wang, M. Transportation Functionality Vulnerability of Urban Rail Transit Networks Based on Movingblock: The Case of Nanjing Metro. *Phys. A Stat. Mech. Its Appl.* **2019**, *535*, 122367. [CrossRef]
23. Shi, J.; Wen, S.; Zhao, X.; Wu, G. Sustainable Development of Urban Rail Transit Networks: A Vulnerability Perspective. *Sustainability* **2019**, *11*, 1335. [CrossRef]
24. Xu, X.; Xu, C.; Zhang, W. Research on the Destruction Resistance of Giant Urban Rail Transit Network from the Perspective of Vulnerability. *Sustainability* **2022**, *14*, 7210. [CrossRef]
25. Fan, Y.; Zhang, F.; Jiang, S.; Gao, C.; Du, Z.; Wang, Z.; Li, X. Dynamic Robustness Analysis for Subway Network With Spatiotemporal Characteristic of Passenger Flow. *IEEE Access* **2020**, *8*, 45544–45555. [CrossRef]
26. Lu, Q.C.; Zhang, L.; Xu, P.C.; Cui, X.; Li, J. Modeling Network Vulnerability of Urban Rail Transit under Cascading Failures: A Coupled Map Lattices Approach. *Reliab. Eng. Syst. Saf.* **2022**, *221*, 108320. [CrossRef]
27. Xiao, X.M.; Jia, L.M.; Wang, Y.H. Correlation between Heterogeneity and Vulnerability of Subway Networks Based on Passenger Flow. *J. Rail Transp. Plan. Manag.* **2018**, *8*, 145–157. [CrossRef]
28. Sun, L.; Huang, Y.; Chen, Y.; Yao, L. Vulnerability Assessment of Urban Rail Transit Based on Multi-Static Weighted Method in Beijing, China. *Transp. Res. Part A Policy Pract.* **2018**, *108*, 12–24. [CrossRef]
29. Zhang, Y.; Ng, S.T. Robustness of Urban Railway Networks against the Cascading Failures Induced by the Fluctuation of Passenger Flow. *Reliab. Eng. Syst. Saf.* **2022**, *219*, 108227. [CrossRef]
30. Pan, S.; Yan, H.; He, J.; He, Z. Vulnerability and Resilience of Transportation Systems: A Recent Literature Review. *Phys. A Stat. Mech. Its Appl.* **2021**, *581*, 126235. [CrossRef]
31. Zhang, S.; Lo, H.K.; Ng, K.F.; Chen, G. Metro System Disruption Management and Substitute Bus Service: A Systematic Review and Future Directions. *Transp. Rev.* **2021**, *41*, 230–251. [CrossRef]
32. Shen, Y.; Ren, G.; Ran, B. Cascading Failure Analysis and Robustness Optimization of Metro Networks Based on Coupled Map Lattices: A Case Study of Nanjing, China. *Transportation* **2021**, *48*, 537–553. [CrossRef]
33. Chen, H.; Zhang, L.; Liu, Q.; Wang, H.; Dai, X. Simulation-Based Vulnerability Assessment in Transit Systems with Cascade Failures. *J. Clean. Prod.* **2021**, *295*, 126441. [CrossRef]
34. Frutos Bernal, E.; Martín del Rey, A. Study of the Structural and Robustness Characteristics of Madrid Metro Network. *Sustainability* **2019**, *11*, 3486. [CrossRef]

35. Chen, H.; Zhang, L.; Ran, L. Vulnerability Modeling and Assessment in Urban Transit Systems Considering Disaster Chains: A Weighted Complex Network Approach. *Int. J. Disaster Risk Reduct.* **2021**, *54*, 102033. [CrossRef]
36. Chen, H.; Chen, B.; Zhang, L.; Li, H.X. Vulnerability Modeling, Assessment, and Improvement in Urban Metro Systems: A Probabilistic System Dynamics Approach. *Sustain. Cities Soc.* **2021**, *75*, 103329. [CrossRef]
37. Nian, G.; Chen, F.; Li, Z.; Zhu, Y.; Sun, D.J. Evaluating the Alignment of New Metro Line Considering Network Vulnerability with Passenger Ridership. *Transp. A Transp. Sci.* **2019**, *15*, 1402–1418. [CrossRef]
38. Han, Y.; Ku, J.; Kim, Y.; Hwang, J. Analyzing the Accessibility of Subway Stations for Transport-Vulnerable Population Segments in Seoul: Case of Bus-to-Subway Transfer. *Case Stud. Transp. Pol.* **2022**, *10*, 166–174. [CrossRef]
39. Yang, T.; Zhao, P.; Qiao, K.; Yao, X.; Wang, T. Vulnerability Analysis of Urban Rail Transit Network by Considering the Station Track Layout and Passenger Behavior. *J. Adv. Transp.* **2021**, *2021*, 6378526. [CrossRef]
40. Zhou, Y.; Wang, J.; Yang, H. Resilience of Transportation Systems: Concepts and Comprehensive Review. *IEEE Trans. Intell. Transp. Syst.* **2019**, *20*, 4262–4276. [CrossRef]
41. Bešinović, N. Resilience in Railway Transport Systems: A Literature Review and Research Agenda. *Transp. Rev.* **2020**, *40*, 457–478. [CrossRef]
42. Serdar, M.Z.; Koç, M.; Al-Ghamdi, S.G. Urban Transportation Networks Resilience: Indicators, Disturbances, and Assessment Methods. *Sustain. Cities Soc.* **2022**, *76*, 103452. [CrossRef]
43. Yin, J.; Ren, X.; Liu, R.; Tang, T.; Su, S. Quantitative Analysis for Resilience-Based Urban Rail Systems: A Hybrid Knowledge-Based and Data-Driven Approach. *Reliab. Eng. Syst. Saf.* **2022**, *219*, 108183. [CrossRef]
44. Wan, C.; Yang, Z.; Zhang, D.; Yan, X.; Fan, S. Resilience in Transportation Systems: A Systematic Review and Future Directions. *Transp. Rev.* **2018**, *38*, 479–498. [CrossRef]
45. Gonçalves, L.; Ribeiro, P. Resilience of Urban Transportation Systems. Concept, Characteristics, and Methods. *J. Transp. Geogr.* **2020**, *85*, 102727. [CrossRef]
46. Zhang, D.M.; Du, F.; Huang, H.; Zhang, F.; Ayyub, B.M.; Beer, M. Resiliency Assessment of Urban Rail Transit Networks: Shanghai Metro as an Example. *Saf. Sci.* **2018**, *106*, 230–243. [CrossRef]
47. Li, M.; Wang, H.; Wang, H. Resilience Assessment and Optimization for Urban Rail Transit Networks: A Case Study of Beijing Subway Network. *IEEE Access* **2019**, *7*, 71221–71234. [CrossRef]
48. Xu, Z.; Chopra, S.S. Network-Based Assessment of Metro Infrastructure with a Spatial–Temporal Resilience Cycle Framework. *Reliab. Eng. Syst. Saf.* **2022**, *223*, 108434. [CrossRef]
49. Xu, Z.; Chopra, S.S.; Lee, H. Resilient Urban Public Transportation Infrastructure: A Comparison of Five Flow-Weighted Metro Networks in Terms of the Resilience Cycle Framework. *IEEE Trans. Intell. Transp. Syst.* **2021**, *23*, 12688–12699. [CrossRef]
50. Chan, H.Y.; Chen, A.; Li, G.; Xu, X.; Lam, W. Evaluating the Value of New Metro Lines Using Route Diversity Measures: The Case of Hong Kong's Mass Transit Railway System. *J. Transp. Geogr.* **2021**, *91*, 102945. [CrossRef]
51. Tang, J.; Xu, L.; Luo, C.; Ng, T.S.A. Multi-Disruption Resilience Assessment of Rail Transit Systems with Optimized Commuter Flows. *Reliab. Eng. Syst. Saf.* **2021**, *214*, 107715. [CrossRef]
52. Ju, Y.; Yuan, H.; Li, Z.; Gan, M.; Chen, Y. Multilayer Structures and Resilience Evaluation for Multimode Regional Rail Transit System. *IET Intell. Transp. Syst.* **2022**, *16*, 843–859. [CrossRef]
53. Liao, T.Y.; Hu, T.Y.; Ko, Y.N. A Resilience Optimization Model for Transportation Networks under Disasters. *Nat. Hazards* **2018**, *93*, 469–489. [CrossRef]
54. Taylor, M. Public Transport Networks. In *Vulnerability Analysis for Transportation Networks*; Elsevier: Amsterdam, The Netherlands, 2017; pp. 175–204.
55. Meng, Y.; Qi, Q.; Liu, J.; Zhou, W. Dynamic Evolution Analysis of Complex Topology and Node Importance in Shenzhen Metro Network from 2004 to 2021. *Sustainability* **2022**, *14*, 7234. [CrossRef]
56. Meng, Y.; Tian, X.; Li, Z.; Zhou, W.; Zhou, Z.; Zhong, M. Exploring Node Importance Evolution of Weighted Complex Networks in Urban Rail Transit. *Phys. A Stat. Mech. Its Appl.* **2020**, *558*, 124925. [CrossRef]
57. Kopsidas, A.; Kepaptsoglou, K. Identification of Critical Stations in a Metro System: A Substitute Complex Network Analysis. *Phys. A Stat. Mech. Its Appl.* **2022**, *596*, 127123. [CrossRef]
58. Freeman, L.C. Centrality in Social Networks Conceptual Clarification. *Soc. Netw.* **1978**, *1*, 215–239. [CrossRef]
59. Freeman, L.C. A Set of Measures of Centrality Based on Betweenness. *Sociometry* **1977**, *40*, 35. [CrossRef]
60. Lin, P.; Weng, J.; Fu, Y.; Alivanistos, D.; Yin, B. Study on the Topology and Dynamics of the Rail Transit Network Based on Automatic Fare Collection Data. *Phys. A Stat. Mech. Its Appl.* **2020**, *545*, 123538. [CrossRef]
61. Hong, J.; Tamakloe, R.; Lee, S.; Park, D. Exploring the Topological Characteristics of Complex Public Transportation Networks: Focus on Variations in Both Single and Integrated Systems in the Seoul Metropolitan Area. *Sustainability* **2019**, *11*, 5404. [CrossRef]
62. Ye, Q.; Kim, H. Partial Node Failure in Shortest Path Network Problems. *Sustainability* **2019**, *11*, 6275. [CrossRef]
63. Ye, Q.; Kim, H. Assessing Network Vulnerability of Heavy Rail Systems with the Impact of Partial Node Failures. *Transportation* **2019**, *46*, 1591–1614. [CrossRef]
64. Meng, Y.; Tian, X.; Li, Z.; Zhou, W.; Zhou, Z.; Zhong, M. Comparison Analysis on Complex Topological Network Models of Urban Rail Transit: A Case Study of Shenzhen Metro in China. *Phys. A Stat. Mech. Its Appl.* **2020**, *559*, 125031. [CrossRef]